A Virtual Screening Approach to Finding Novel and Potent Antagonists at the Melanin-Concentrating Hormone 1 Receptor

David E. Clark,* Christopher Higgs, Stephen P. Wren, Hazel J. Dyke, Melanie Wong, Dennis Norman, Peter M. Lockey, and Alan G. Roach

Argenta Discovery Ltd., 8/9 Spire Green Centre, Flex Meadow, Harlow, Essex, CM19 5TR, U.K.

Received January 5, 2004

Melanin-concentrating hormone (MCH) has been known to be an appetite-stimulating peptide for a number of years. However, it is only recently that MCH has been discovered to be the natural ligand for a previously "orphan" G-protein-coupled receptor, now designated MCH-1R. This receptor has been shown to mediate the effects of MCH on appetite and body weight, and consequently, drug discovery programs have begun to exploit this information in the search for MCH-1R antagonists for the treatment of obesity. In this paper, we report the rapid discovery of multiple, structurally distinct series of MCH-1R antagonists using a variety of virtual screening techniques. The most potent of these compounds (**12**) demonstrated an IC_{50} value of 55 nM in the primary screen and exhibited antagonist properties in a functional cellular assay measuring Ca^{2+} release. More potent compounds were identified by follow-up searches around the initial hit. A proposed binding mode for compound **12** in a homology model of the MCH-1R is also presented.

Introduction

Obesity is a chronic disorder in which there is an imbalance between energy intake and expenditure; specifically, a long-term excess of energy (food) intake over energy expenditure leads to an excess in white adipose tissue mass. The prevalence of obesity has increased dramatically in recent years such that it is now recognized as a serious medical problem, particularly in the Western world.[1,2] Obesity is now accepted as a major risk factor for non-insulin-dependent (type 2) diabetes, hypertension, peripheral and coronary vascular disease, stroke, various musculoskeletal disorders, and certain cancers. In response to the pronounced trend of increasing obesity among the population of the developed world, the pharmaceutical industry has embarked upon various strategies for drug intervention, primarily targeting the reduction of energy intake.[3−5]

The regulation of food intake by mechanisms in the central nervous system (CNS) has been heavily researched over the past few decades.[6] As a result of this extensive research, a large number of peptide and nonpeptide neurotransmitters have been shown to modify feeding behavior via several G-protein-coupled receptors (GPCRs).[7,8] The evidence for melanin-concentrating hormone (MCH), a cyclic 19 amino acid neuropeptide, regulating food intake and energy homeostasis has been reviewed comprehensively.[9] In 1999, the orphan SLC-1 receptor was identified as the MCH receptor and redesignated the MCH-1 receptor (MCH-1R).[10,11]

MCH-1R has been implicated in the control of energy intake by a variety of studies. By use of peptide analogues of MCH that act as agonists at the MCH-1R, it was shown that stimulation of this receptor was correlated with an increase in food intake in the rat.[12] More recently, other work in rats employing an MCH-1R agonist confirmed these findings.[13] The same group also investigated the effect of a MCH-1R antagonist and showed that continuous antagonism of the receptor led to sustained reductions in food intake, weight, and fat gain compared to the control animals.[13] Other workers studying the actions of MCH-1R antagonists in animal models have reported similar results.[14,15] Intriguingly, the latter report suggests that MCH-1R may also be a target for the development of anxiolytics and antidepressants.

In a knockout study, MCH-1 receptor deficient mice (mch1r−/−) were created and it was shown that although they had normal body weights, they were lean with a reduced fat mass.[16] Surprisingly, the mch1r−/− mice were hyperphagic when maintained on normal chow leading to the conclusion that their leanness was a consequence of hyperactivity and/or altered metabolism. Further to this observation, the mch1r−/− mice were resistant to diet-induced obesity compared to wild-type mice and, unlike wild-type mice, chronic central infusions of MCH failed to induce hyperphagia and mild obesity. Therefore, it was concluded that MCH-1 receptors are physiologically relevant in energy homeostasis in mice through multiple actions on appetite, locomotor activity, metabolic rate, and neuroendocrine function.[16] The ultimate validatory information linking MCH (and MCH-1R) to a modifying role in obesity will be generated with small-molecule antagonists given in a clinical setting. There is thus currently great interest in the identification of compounds with appropriate activity, selectivity, and pharmacokinetic properties to permit such tests to take place.[17,18]

In this paper, we report the discovery of multiple, structurally distinct series of MCH-1R antagonists using a number of virtual screening methods. In what follows,

* To whom correspondence should be addressed. Phone: +44 (0) 1279 645 611. Fax: +44 (0) 1279 645 646. E-mail: david.clark@argentadiscovery.com.

10.1021/jm040762v CCC: $27.50
Published on Web 07/02/2004

we describe first the strategy for virtual screening and the selection of a subset of compounds for biochemical screening from the virtual hits identified thereby. The screening results are then presented, and early structure−activity relationships (SAR) identified by means of screening additional compounds similar to the most potent hit are described. The construction of a homology model of the MCH-1R is reported together with a putative binding mode for one of the potent antagonists identified in this work. Finally, we discuss the virtual screening results examining the success rates of the various techniques employed.

Virtual Screening

Following a review of the literature concerning MCH-1R antagonists, 11 compounds were chosen as the basis for virtual screening (Figure 1 and Table 1). All searches were carried out within (a subset of) a database of approximately 615 000 commercially available screening compounds collated in-house from supplier catalogues. All compounds in this database had passed multiple in silico filters aimed at removing nondruglike molecules prior to virtual screening.

Conventional wisdom dictates that there is value in applying as many virtual screening techniques as possible to a given problem, since each search type typically returns a different set of hit structures.[27] Consequently, 2-D substructure, 2-D similarity, 3-D similarity, and 3-D substructure searches were carried out using the 11 compounds in Figure 1 as the basis for queries. Additionally, some of the 11 compounds were manually docked into an MCH-1R homology model (vide infra) and structure-directed pharmacophore searches were carried out on the basis of their docked conformations. Finally, a clustering approach was used to select further compounds that may have been missed by the other searches.

From all the searches, 3015 hits were selected for further analysis in conjunction with an experienced medicinal chemist. The compounds were assessed on their druglikeness and synthetic tractability and also in terms of a number of key computed properties such as molecular weight (MW), ClogP,[28] and polar surface area (PSA); 2018 compounds were selected as being suitable for purchase. A number of compounds appeared as hits from multiple searches. When these duplicates were removed, 1490 unique compounds remained. This set of compounds was then clustered using Ward's method[29] based on Daylight fingerprints and a Tanimoto similarity threshold of 0.85, which yielded 874 clusters. From a visual inspection of these clusters, 877 compounds were selected for purchase. After investigation of availability and price, 806 compounds were ordered of which 795 were received.

Biochemical Screening Results

A scintillation proximity assay using ^{125}I-[Phe^{13},Tyr^{19}]-MCH binding to MCH-1R membranes was developed. The 795 selected compounds were initially tested at a single concentration (10 μM). This resulted in 62 actives (showing >40% inhibition), which were retested in duplicate at 10 μM. On the basis of the duplicate screening results, IC_{50} values were determined for 19 compounds (six-point curves). Of the 19 compounds, four had IC_{50} values below 1 μM, four were in the range 1−10 μM, and the remaining 11 were in the range 11−30 μM. Following the IC_{50} determinations, seven compounds representing the heads of seven structurally distinct hit series were selected for further assessment. The investigation of one of these hit series is described below.

The most potent compound (**12**, Figure 2, Table 2) in this series was found to have an IC_{50} value in the binding assay of 55 nM. Compound **12** was evaluated in a functional assay measuring Ca^{2+} release. No agonist activity, defined as a release of Ca^{2+}, was observed, and the compound was able to inhibit the effect of 0.1 μM MCH (EC_{80}). Scatchard analysis in the binding assay demonstrated that the compound was a competitive antagonist. As well as being a reasonably potent antagonist at the MCH-1R, compound **12** has attractive computed physicochemical properties (MW = 424.9, PSA = 64.5 Å^2, ClogP = 4.47) together with some obvious synthetic disconnections. It was thus considered to be an excellent starting point for hit-to-lead optimization studies.[30]

Structure−Activity Relationships

Some early SAR data were obtained around compound **12** in the first round of screening and are summarized in Table 2. To expand upon this, further 2-D similarity and substructure searches were conducted around compound **12** and seven additional compounds were purchased and screened in the primary assay. The results of this are summarized in Table 3. In terms of SAR, the following can be deduced.

(1) The Me/Et switch at R1 does not affect activity significantly (compare compounds **12** and **16**).

(2) The methyl substitution in the linker in R2 has a detrimental effect (compare compounds **15** and **17**). However, there are no data to prove if this would also be the case in compounds lacking an ortho substituent on the terminal aromatic ring in which the conformational effect may be less marked.

(3) An aromatic group at the R2 terminus appears to be necessary for good activity, since the change to an aliphatic group at the terminus (compound **21**) produces a poorly active compound.

(4) A para substituent in the terminal aromatic group seems to be required for potency. Lipophilic substituents, like chloro, seem to give better potency than the more polar methoxy.

Compounds **15** (IC_{50} = 18 nM) and **16** (IC_{50} = 37 nM) show greater potency than **12**, and the former represents the most potent compound identified in this work. However, the introduction of the additional chloro substituent does raise the ClogP value of **15** to 5.00, which may be considered a little high for an early stage compound.

Homology Model of MCH-1R and Binding Mode for Compound 12

The crystal structure of rhodopsin[31] determined at 2.6 Å was used as the template for a model of the transmembrane helical region of the MCH-1R. Comparison of the resulting MCH-1R homology model with the rhodopsin crystal structure, shown in Figure 3, revealed very little difference in the position and tilt of the backbone, with only helix 4 moving slightly outward.

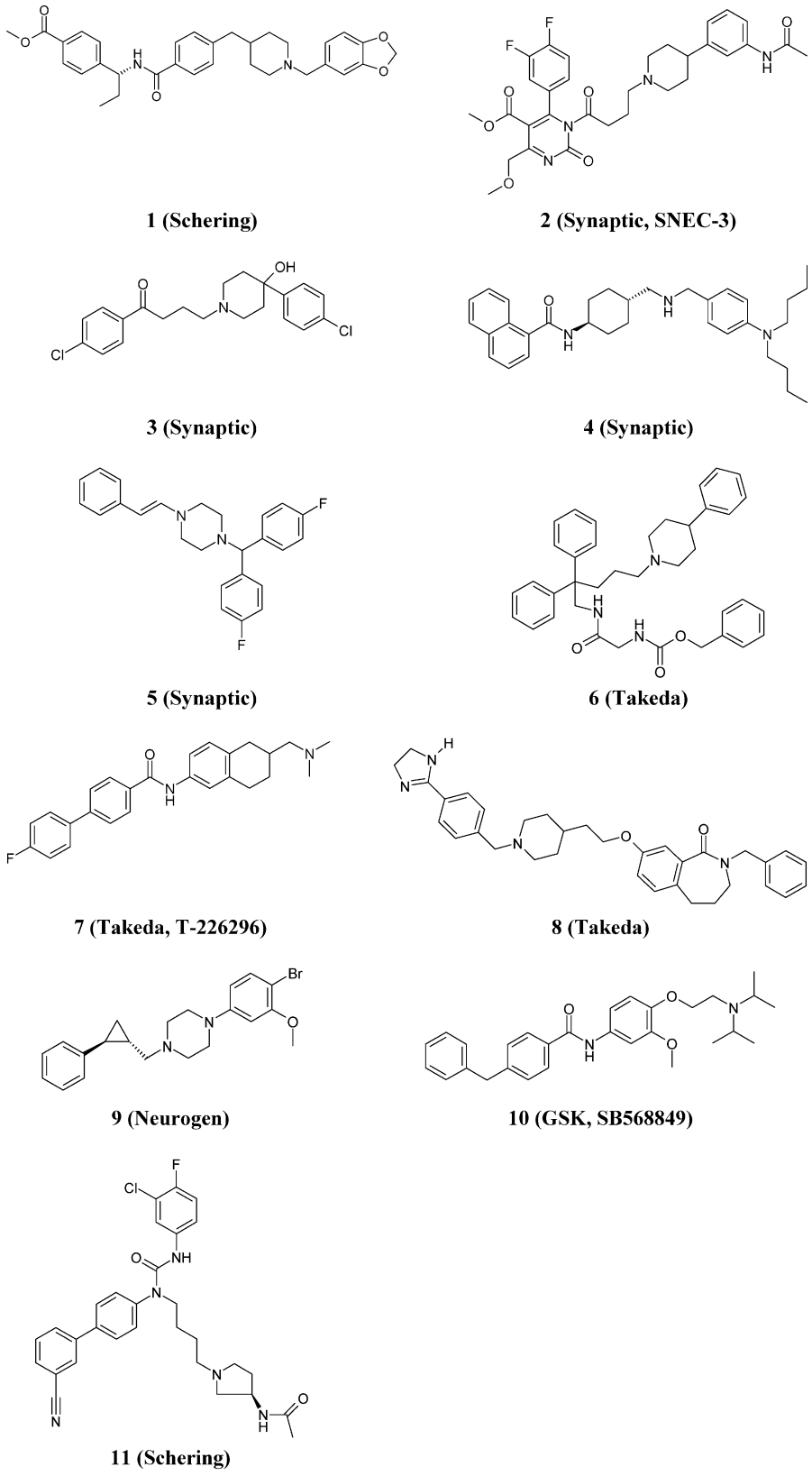

Figure 1. The 11 compounds selected as the basis for virtual screening.

Compound **12** was then manually docked into this model, and the resulting complex was subjected to energy minimization. The proposed binding mode is shown from different perspectives in Figures 4 and 5.

In this binding mode, compound **12** appears to make three key interactions with the postulated receptor binding site. First, a salt bridge formed between the tertiary amine of the piperazine moiety and Asp172, which is located at the extracellular end of helix 3. In mutagenesis studies, the mutation D172A completely abolished MCH (agonist) binding, showing this residue to be critically important in the formation of the MCH peptide/receptor complex.[32] Interestingly, Asp172 is in a position identical to that of the critical Asp residue

Table 1. Published MCH-1R Affinity Data for Query Compounds

compd	published MCH-1R affinity	ref
1	$K_i \leq 1.5\ \mu M$	19
2	$K_b = 0.57$ nM	20
3	$K_b = 9$ nM	21
4	$K_b = 284$ nM	21
5	$K_b = 260$ nM	21
6	$IC_{50} = 5$ nM	22
7	$IC_{50} = 5.5$ nM	14
8	$IC_{50} = 300$ nM	23
9	$K_i < 1\ \mu M$	24
10	$K_i = 40-79$ nM	25
11	$K_i < 100$ nM	26

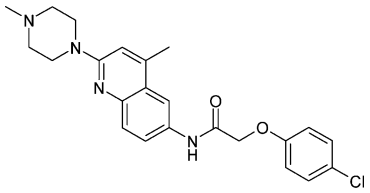

12

Figure 2. Most potent compound identified by the initial round of virtual screening.

Table 2. Early SAR Data from the First Round of Compound Screenings

Common Core	Compound	R1	R2	IC_{50} (μM)
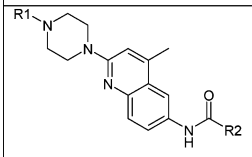	**12**	Me	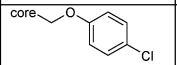	0.055
	13	Et	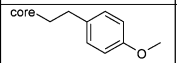	0.73
	14	Et	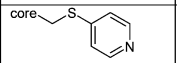	8.2

found in the biogenic amine receptors. The amide carbonyl of **12** forms a hydrogen bond with the side chain of Gln325 located on helix 6, and the terminal chlorophenyl moiety is situated in an aromatic binding region comprising a number of phenylalanine residues from helices 5 and 6.

Discussion

It is interesting to analyze which searches gave rise to which hit compounds. Table 4 collates this information for the 19 compounds for which IC_{50} values were determined. There are several points of note. First, of the 11 compounds used as queries, only two (compounds **5** and **6**) did not give rise to any of the hits. This suggests that when carrying out ligand-based screening, it is advantageous to use as many query compounds as possible to maximize the chances of finding hits. Second, nearly half of the compounds (9/19) were selected from two or more different searches, while the remainder originated from only one search. There appears to be no simple relationship between a compound's activity and the number of searches in which it was retrieved.

Table 5 presents the results of an analysis of the success rates of the different search types employed. The first column shows the number of compounds screened

Table 3. Additional SAR Data around Compound **12**

Common Core	Compound	R1	R2	IC_{50} (μM)
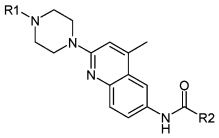	**15**	Me	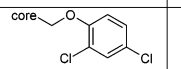	0.018
	16	Et	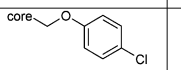	0.037
	17	Et	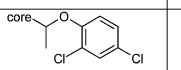	0.23
	18	Me	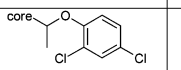	0.79
	19	Me	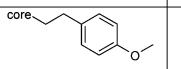	0.25
	20	Et	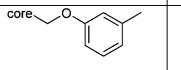	6.6
	21	Me	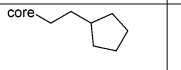	11.6% inhib. @ 10μM

that were found by a particular search type (note that the total in this column exceeds 795 because many compounds were found by more than one search type, as discussed above). The second column shows how many of the compounds in Table 4 were found by each search type, and the hit rate is the ratio of these two numbers. The results indicate that in this instance the 2-D similarity searches have been the most effective, with a hit rate of 5.6%. The 3-D substructure searches also yielded a good hit rate (4.3%), with clustering and FlexS performing less well but still respectably (2.4% and 2.1%, respectively). The 2-D substructure searches and the site-directed pharmacophore searches did not give rise to any of the compounds in Table 4 and so are judged to have been unsuccessful in this case. Whether this lack of success is due to shortcomings in the application of these methodologies or is simply a function of chance and the relatively small numbers of compounds screened from these two search types is impossible to determine. The overall figures do, however, disguise the fact that all the compounds with submicromolar activity resulted from 3-D searches. Additionally, the hit rate of a search is only one measure of its value and can easily be biased by the presence of analogue series in a database. It is our contention that ultimately the real value of a virtual screening search can only be judged in terms of whether it yields (a series of) compounds that are judged to be suitable starting points for medicinal chemistry optimization. Such a judgment involves the consideration of many factors in addition to biological potency, some of which are subjective in nature, such as synthetic tractability and the potential for obtaining a secure patent position.

One might expect the 3-D search types, FlexS, and 3-D substructure to be more effective at "lead hopping", i.e., locating compounds with novel scaffolds but showing the same biological activity as known actives. Nonetheless, it is clear that the simple and rapid 2-D similarity searches should not be discounted because

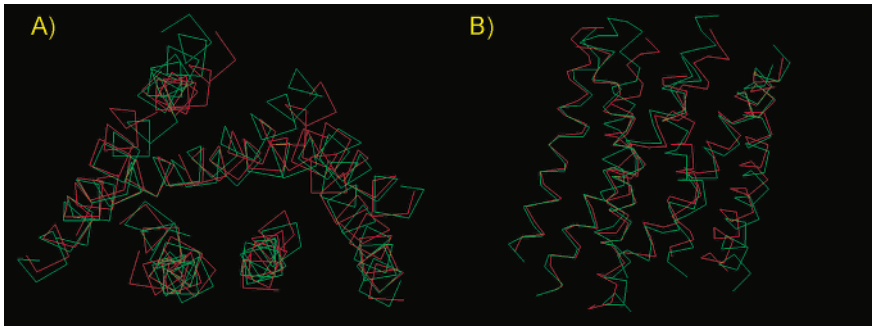

Figure 3. Comparison of the MCH-1R homology model (green) with the rhodopsin crystal structure (red) as viewed from (A) the extracellular domain in a counterclockwise direction and (B) perpendicular to the membrane.

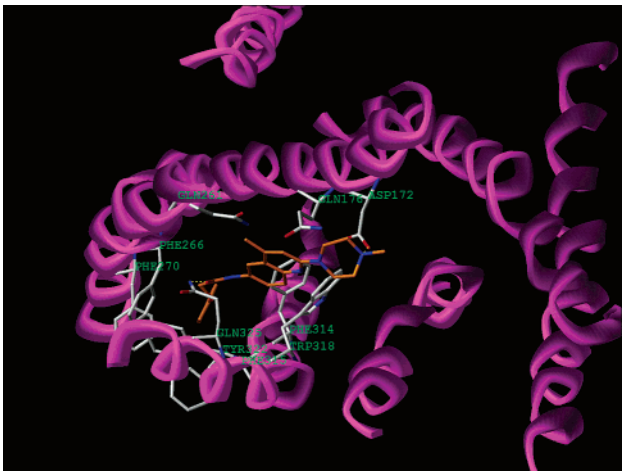

Figure 4. Proposed binding mode of **12** in homology model of MCH-1R viewed from the extracellular domain.

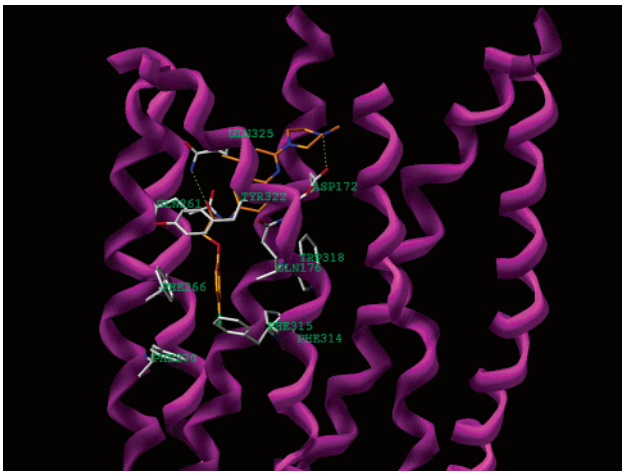

Figure 5. Proposed binding mode of **12** in homology model of MCH-1R viewed from the perpendicular to the membrane.

they are capable of yielding high hit rates and, in this case, were uniquely responsible for the identification of compound **F** in Table 4. Similarly, the clustering exercise proved to be fruitful in identifying active compounds not discovered by other methods. Although methods based on 2-D structure are more likely to retrieve structures with a high scaffold similarity to the query compound, there is always potential at lower similarity values for finding compounds not covered by the scope of a competitor's patent or from which a novel position can be obtained. Overall, our findings bear out the value of employing multiple search types in ligand-based virtual screening.[27]

Table 4. Virtual Screening Searches Giving Rise to the 19 Compounds for Which IC_{50} Values Were Determined[a]

compd	IC_{50} (μM)	search 1	search 2	search 3	search 4
A (**12**)	0.055	10_3d_sub	10_flexs		
B	0.70	3_flexs			
C (**13**)	0.73	10_flexs	8_flexs		
D	0.82	3_3d_sub	9_3d_sub		
E	1.8	4_flexs			
F	2.9	4_2d_sim			
G	4.0	1_3d_sub	11_3d_sub		
H (**14**)	8.2	clustering	10_flexs		
I	11.0	1_3d_sub	3_flexs	8_flexs	
J	11.4	1_3d_sub	10_3d_sub		
K	12.9	2_3d_sub	9_2d_sim		
L	12.9	7_flexs			
M	14.5	10_flexs			
N	14.7	clustering			
O	18.1	2_flexs			
P	19.9	1_3d_sub	3_3d_sub	10_3d_sub	11_3d_sub
Q	24.0	clustering			
R	25.0	10_3d_sub			
S	26.7	1_3d_sub			

[a] In the notation in the table, a search is denoted by the compound upon which it was based (numbers as in Figure 1) and the search type, with the exception of clustering, which was not based on any compound. "flexs" = FlexS (3-D similarity). "3d_sub" = 3-D substructure. "2d_sim" = 2-D similarity.

Table 5. Hit Rates of the Various Types of Search in Terms of the Number of Compounds Selected for IC_{50} Determination Compared to the Number of Compounds Screened

search type	no. of compds screened	no. of hits in Table 4	hit rate (%)
flexs	526	11	2.1
3d_sub	350	15	4.3
2d_sub	11	0	0.0
2d_sim	36	2	5.6
clustering	124	3	2.4
structure-directed pharmacophore	49	0	0.0

Finally, it is noteworthy that the hit-finding project described in this work was conducted in 6 months, including the time required to obtain the compounds from the commercial sources, and used relatively little resource, particularly in terms of synthetic or medicinal chemistry (note that all compounds reported in this paper are commercially available). While reports are beginning to appear in the literature that indicate that virtual screening using GPCR homology models can be successful,[33,34] the results reported here demonstrate that ligand-based virtual screening is also an efficient and cost-effective approach to hit-finding against GPCR targets. Others have reported similar successes against, for instance, the urotensin II receptor,[35] the dopamine D3 receptor,[36] and the adenosine A_{2A} receptor.[37] This

Table 6. Compound Suppliers Whose Collections Were Used To Create the Database in This Work

supplier	no. of compds (as of May 2002)	URL
Abinitio Pharmasciences	42017	http://www.abinitiopharma.com
AF ChemPharm	372	http://www.afchempharm.co.uk
ASDI	32496	http://www.asdi.net
ASINEX	264169	http://www.asinex.com
Bionet Research	33062	http://www.keyorganics.ltd.uk
ChemBridge	232460	http://www.chembridge.com
ChemDiv	338003	http://www.chemdiv.com
ChemStar	63697	http://www.chemstaronline.com
Comgenex	75942	http://www.comgenex.com
Evotec OAI	62418	http://www.evotecoai.com
I. F. Lab	92812	http://www.iflab.kiev.ua
InterBioScreen	192895	http://www.ibscreen.com
Labotest	48594	http://www.labotest.com
Maybridge	56159	http://www.maybridge.com
Molecular Design and Discovery	26848	http://www.worldmolecules.com
Otava	92510	http://www.otava.com.ua
Peakdale	749	http://www.peakdale.co.uk
Pharmacore	17600	http://www.pharmacore.com
Petrenko (University of Kiev)	89249	N/A
Specs	141021	http://www.specs.net
Timtec	71321	http://www.timtec.net
Tocris	802	http://www.tocris.com
TOSLab	6651	http://www.toslab.com
Vitas-M	53531	http://www.vitasmlab.com

type of virtual screening approach has become a core component of our hit-finding capabilities, and further successful applications of it will be reported in due course.

Summary

In this paper, we have presented the results of a hit-finding program against the MCH-1R using a variety of virtual screening approaches. In a short time period, we were able to discover seven structurally diverse series of hit compounds, including compound **12**, which gave an IC_{50} value of 55 nM in the primary assay and was subsequently demonstrated to be a competitive antagonist of the MCH-1R. Follow-up searches around this compound yielded additional potent compounds and some early SAR. Hit-to-lead chemistry exploration around this compound will be reported elsewhere.[30] An analysis of the virtual screening results confirmed the conventional wisdom of utilizing as many query compounds and search techniques as possible in order to maximize the chances of finding hits.

Methods

1. Database Construction. The electronic catalogues (SD files) of 24 screening compound suppliers were collated, giving an initial total of just over two million compounds (see Table 6). This set was then processed to remove duplicates and compounds possessing undesirable or reactive substructures (such as those specified by Rishton[38,39] and Hann et al.[40]) or having key molecular properties outside specified ranges (see Table 7). At the end of the filtering process, approximately 615 000 compounds remained. From this set of compounds, three kinds of database were constructed for use in virtual screening. In all the databases, compounds were stored in their neutral forms and the 11 query compounds were represented in the same manner.

1.1. Daylight Database. A fingerprinted TDT file for use with programs based on the Daylight toolkit.[42]

1.2. Unity Database. Constructed from 3-D structures generated by Concord[43] and for use with the Unity database searching program.[44]

1.3.1. FlexS Database 1. A subset of approximately 13 600 compounds from the Unity database was created for use with the FlexS program.[45,46] This subset was derived from the larger database by selecting only tertiary amines satisfying the following criteria: (1) number of aromatic rings of 2−4; (2) molecular weight of 300−450; (3) number of rotatable bonds les than 7.

Table 7. Criteria Used for Computational Filtering of Commercial Compound Collections[a]

computed molecular property	value
minimum allowed molecular weight	200.0
maximum allowed molecular weight	550.0
minimum allowed number of rings	1
maximum allowed number of rings	5
minimum allowed ring size	3
maximum allowed ring size	8
minimum allowed number of heavy atoms	10
maximum allowed number of heavy atoms	100
minimum hetero to heavy atom ratio[a]	0.1
maximum hetero to heavy atom ratio	0.5
maximum number of halogens	6
maximum number of fluorines	4
maximum number of chlorines	2
maximum number of bromines	1
maximum number of sulfurs	2
minimum number of rotatable bonds	0
maximum number of rotatable bonds	10
maximum number of rings in a fused ring system	3
Delete molecules containing only aromatic atoms?	yes
Delete molecules failing Lipkus criteria?[b]	yes

[a] The hetero to heavy atom ratio is computed as the number of non-carbon heavy (i.e., not hydrogen) atoms divided by the total number of heavy atoms in a molecule and is intended to eliminate molecules that are either under- or overfunctionalized. [b] The Lipkus filter is intended to remove compounds containing rings that are not "medicinally relevant", typically unusual bridged or caged structures, and is based on the work described in ref 41.

1.3.2. FlexS Database 2. A smaller subset of FlexS database 1 was created by applying the following additional criteria: (1) molecular weight greater than 360; (2) topological polar surface area[47,48] less than 100 Å^2. All FlexS database compounds were energy-minimized using the MMFF94s force field as implemented in Sybyl.[49]

2. Virtual Screening. In conjunction with the databases described above, six approaches were used to select compounds as potential candidates for purchase. In most cases, all searches were conducted for each query compound except for instances in which time constraints made this impossible or when it was felt that a particular search would not be worthwhile for a particular compound. The exception was the

Table 8. Database Searches That Were Carried Out for Each Query Compound[a]

query compd	2-D substructure	2-D similarity	3-D substructure	3-D similarity
1	×	√	√	√
2	×	×	√	√
3	×	√	√	√
4	×	√	√	√
5	×	√	√	√
6	×	√	√	×
7	√	√	√	√
8	×	√	√	√
9	×	√	√	√
10	×	√	√	√
11	×	√	√	×

[a] √ denotes that a particular search was carried out; × denotes the opposite.

2-D substructure searches, which were quickly abandoned as being of limited use. The types of search for which each query compound was used are summarized in Table 8.

2.1. 2-D Substructure Searches. Carried out using Daylight SMARTS[42] queries.

2.2. 2-D Similarity Searches. Four kinds of similarity search were used employing Daylight fingerprints (Tanimoto similarity coefficient),[42] Unity fingerprints (Tanimoto and cosine similarity coeffients),[44] and an in-house program based on Daylight fingerprints but using a data fusion approach to combine Tanimoto and Russell−Rao similarity coefficients.[50] For the Daylight and Unity searches, similarity thresholds were set pragmatically such that a manageable number of hits was returned from each search (typically a few tens of compounds). In general, Tanimoto coefficients in the range 0.7−0.85 and cosine coefficients in the range 0.8−0.9 were found to be effective. The in-house data fusion program returns a specified number of most similar compounds; this number was generally chosen to be similar to the number of hits obtained from the Daylight and Unity searches.

2.3. 3-D Similarity Searches. FlexS[45,46] was used in its Flexible Superposition mode. Default settings were maintained except that the charges used for the database compounds were those from the MMFF94s force field and only three alignments per ligand were generated. A low-energy conformation of the query molecule for use as the template in a FlexS search was typically identified by a LowMode conformational search using the MMFFs force field and GB/SA continuum solvent (water) model as implemented in Batchmin.[51] Typically the top 300 compounds according to the FlexS normalized and total scores (i.e., 600 compounds in total) were visually inspected. Those overlaying well with the query molecule were selected for further consideration.

2.4. 3-D Substructure Searches. Unity[44] was used for all 3-D substructure searches. Typically, these searches involved three- or four-point queries always including the amine presumed to be important for activity and a hydrophobic center presumed to bind in the aromatic binding region near helices 5 and 6. Distance ranges between query features were derived from monitoring the interfeature distances during conformational analyses using the CSEARCH module of Sybyl.[49] A torsion angle increment of 30° was used for most compounds with a 60° increment being used for compounds with a larger number of rotatable bonds.

2.5. Structure-Based Pharmacophore Searches. An alignment of 10 of the compounds in Figure 1 was generated by manually docking them into the initial version of the homology model described below (compound **9** was not included because its binding mode could not be predicted with any confidence). The only experimental evidence available to guide this process was the knowledge that the mutation D172A completely abolishes MCH (agonist) binding, showing this residue to be critically important in the formation of the MCH peptide/receptor complex.[32] Compound **7** was docked first, placing the basic amine moiety to interact with Asp172. The rest of the compound was then positioned to allow the terminal hydrophobic moiety to occupy an aromatic binding region comprising a number of phenylalanine residues from helices 5 and 6. This initial complex was refined using simulated annealing. During this simulation, the protein backbone was held fixed but movement was observed in the side chains, which moved to "open up" the binding site by comparison to the rhodopsin template. The starting positions for the other nine compounds were generated by overlaying them on the docked conformation of compound **7** using GASP[52,53] with the initial complexes being refined by simulated annealing. Comparison of these complexes after simulated annealing revealed that there was very little change in the side chain positions regardless of which ligand was in complex with the receptor.

On the basis of this alignment, three pharmacophores were derived for use as Unity search queries.[44]

(1) Based on the docked structure of compound **7** incorporating four points: positive N, hydrogen-bond acceptor, and two hydrophobes.

(2) Based on the docked structures of compounds **6** and **10**, comprising three points: positive N, hydrogen-bond acceptor, and hydrophobic.

(3) Based on docked structures of compounds **6** and **7**, comprising three points: positive N and two hydrophobic.

2.6. Clustering. Finally, given the imperfections in all virtual screening approaches, it was decided to include a clustering selection of compounds in addition to the more directed searches above. A subset of approximately 2850 compounds was derived from FlexS database 2 by the removal of compounds already selected for purchase and the application of further molecular property filters including the removal of compounds satisfying any of the following criteria:

(a) ClogP: <2.5 or >5.5

(b) topological PSA: >90 Å^2

(c) predicted log BB: less than -0.5 (computed using an in-house model based on ref 54)

(d) predicted log *S*: less than -7.0 (as computed by QikProp[55])

(e) number of halogens: >2

(f) number of rings: <3

(g) number of rotatable bonds: >6

The set of 2850 compounds was clustered using Ward's method[29] based on Daylight fingerprints[42] at a Tanimoto similarity threshold of 0.8. This resulted in 716 clusters, and the compound closest to the center of mass of each cluster was considered for purchase.

3. Follow-Up Searches. To find follow-up compounds around compound **12**, multiple similarity searches were carried out, together with a specific substructure search for compounds containing a similar scaffold. Specifically, the following types of similarity search were performed.

(a) Daylight fingerprint-based[42] using the Tanimoto similarity coefficient typically at a threshold of 0.8.

(b) Unity fingerprint-based[44] using the Tanimoto similarity coefficient typically at a threshold of 0.8.

(c) Atom pairs-based[56] using the Tanimoto similarity coefficient. This method is encoded in an in-house program that returns a specified number of hits. This number was typically chosen on the basis of the number of hits obtained in the Daylight and Unity similarity searches.

(d) Feature trees similarity-based using the FTrees program.[57,58] In this case, the same number of hits as for the atom pair-based program was selected for visual inspection.

4. Homology Modeling. The MCH-1R is a class A rhodopsin-like G-protein-coupled receptor. To help in the discovery of MCH-1R antagonists, it was decided to construct a homology model of the transmembrane helices of the receptor. The crystal structure of rhodopsin used in this work, 1L9H,[31] is believed to be in the inactive form. It is therefore natural to assume that this structure is more suited to the design of antagonists than agonists.[59] The MCH-1R model was constructed by initially mutating the rhodopsin crystal structure to a polyalanine model. Each helix in turn was then mutated to the corresponding MCH-1R sequence using the Biopolymer CHANGE command within Sybyl[49] according to the sequence

```
MCH1R   MSVGAMKKGVGRAVGLGGGSGCQATEEDPLPNCGACAPGQGGRRWRLPQPAWVEGSSARL

Rhod    ------------------------------------------------------------

MCH1R   WEQATGTGWMDLEASLLPTGPNASNTSDGPDNLTSAGSPPRTGSISYINIIMPSVFGTIC

Rhod    ----------------------------------------------WQFSMLAAYMFLLI

MCH1R   LLGIIGNSTVIFAVVKKSKLHWCNNVPDIFIINLSVVDLLFLLGMPFMIHQLMGNGVWHF

Rhod    MLGFPINFLTLYVTVQ---------PLNYILLNLAVADLFMVFGGFTTTLYTSLH-----

MCH1R   GETMCTLITAMDANSQFTSTYILTAMAIDRYLATVHPISSTKFRKPSVATLVICLLWALS

Rhod    -PTGCNLEGFFATLGGEIALWSLVVLAIERYVVV------------NHAIMGVAFTWVMA

MCH1R   FISITPVWLYARLIPFPGGAVGCGIRLPNPDTDLYWFTLYQFFLAFALPFVVITAAYVRI

Rhod    LACAAPPLV-----------------------NESFVIYMFVVHFIIPLIVIFFCYGQ-

MCH1R   LQRMTSSVAPASQRSIRLRTKRVTRTAIAICLVFFVCWAPYYVLQLTQLSISRPTLTFVY

Rhod    -------------------EKEVTRMVIIMVIAFLICWLPYAGVAFYIFT---------I

MCH1R   LYNAAISLGYANSCLNPFVYIVLCETFRKRLVLSVKPAAQGQLRAVSNAQTADEERTESK

Rhod    FMTIPAFFAKTSAVYNPVIY----------------------------------------

MCH1R   GT

Rhod    --
```

Figure 6. Alignment of the sequences of bovine rhodopsin and the human MCH-1R. Key sequence motifs used to align the sequences are shown in bold. Only the sequence for the transmembrane helical region of rhodopsin is given.

alignment shown in Figure 6. This alignment was generated manually by aligning key class A sequence motifs (shown in bold in Figure 6) in the two sequences. The lengths of the transmembrane helices were as defined by Palczewski et al.,[60] and the sequence identity between the MCH-1R and rhodopsin sequences in the transmembrane helical regions is 21.1%. Next, the side chains were minimized using the Tripos force field as implemented in Sybyl.[49] Side chain rotamers for highly conserved residues that pointed into the binding pocket were manually corrected in cases in which they differed significantly from those observed in the rhodopsin structure and then reminimized. This process was repeated for each helix.

For the vast majority of residues, the side chains exhibited rotamer angles very similar to those observed in rhodopsin, and these were maintained through the minimization process. However, two problematic positions, Tyr322 and Gln176, were identified. Initially, Tyr322, found on helix 6, was orientated into the aromatic pocket, limiting its size. However, this side chain could easily be orientated to face either inward or outward and no indication of the side chain's orientation can be drawn from the rhodopsin structure because the corresponding residue is an alanine. Therefore, Tyr322 was orientated outward to "open up" the aromatic pocket. In its initial orientation, Gln176 was found to be forming a hydrogen bond with Asp172. However, to maintain this interaction during energy minimization, Trp318, on helix 7, rotated toward the aromatic pocket. Because this residue is conserved in both rhodopsin and MCH-1R, the rotamer angles were maintained for Trp318 while Gln176 was moved, breaking the hydrogen bond to Asp172 and allowing Trp318 to remain in a position similar to that observed in the rhodopsin crystal structure.

A fundamental principle of homology modeling is that the proteins share a common fold. Indeed, it is widely accepted that G-protein-coupled receptors fold in the same way. However, although it is assumed that each of the seven transmembrane domains folds to form an α-helix, the mobility and flexibility of each helix can differ between various receptors. This is due, at least in part, to the varying position of proline and glycine residues in each helix. An analysis of the sequence alignment between rhodopsin and MCH-1R identified possible regions of differing flexibility and rigidity. To incorporate the flexibility of proline and glycine residues, the model was minimized with harmonic constraints placed between C═O(i) and NH($i + 4$) of the backbone. The purpose of the constraints was to maintain an existing hydrogen bond, remove flexibility due to the removal of a proline or glycine residue, or incorporate flexibility due to the introduction of proline or glycine residue. However, before the flexibility/rigidity was incorporated, the side chains underwent simulated annealing, using the MMFFs force field as implemented in Macromodel,[51] to remove any remaining steric clashes because these could exaggerate the movement of the helices during the minimization of the backbone.

Finally, the side chains of the resulting minimized structure underwent simulated annealing (MMFFs force field, Macromodel[51]) to relieve any steric clashes and correct unfavorable torsion angles. The resulting model satisfied the protein geometry checker embodied within Sybyl[49] (ProTable), which identifies improper bond lengths and torsion angles.

5. Biochemical Assays. 5.1. MCH-1R Scintillation Proximity Assay. Chinese hamster ovary (CHO) cell membranes (5μg) overexpressing the MCH-1R (Euroscreen S.A.) were incubated with 25 μg of wheat germ agglutinin SPA beads (Amersham Biosciences UK Ltd.) and 0.4 nM ^{125}I-[Phe^{13}, Tyr^{19}]-MCH (Amersham Biosciences U.K. Ltd.) in a final volume of 100 μL of binding buffer (25 mM HEPES, 10 mM NaCl, 5 mM $MgCl_2$, 1 mM $CaCl_2$, 0.1% BSA) containing 5 mM phosphoramidon for 1 h at room temperature. Nonspecific binding was determined in the presence of 1 μM MCH (Bachem (U.K.) Ltd). Bound ^{125}I-[Phe^{13}, Tyr^{19}]-MCH was detected using a MicroBeta TRILUX liquid scintillation counter (Perkin-Elmer). Compound IC_{50} was determined using a six-point concentration−response curve with a semilog compound dilu-

tion series. IC_{50} calculations were performed using Excel and XL fit (Microsoft).

5.2. Ca^{2+} Mobilization Assay. Stable CHO-K1 cells overexpressing the MCH-1R were seeded (35 000 cells per well with a plating volume of 50 μL) into collagen-coated 96-well plates 24 h prior to the assay. The cells were then loaded with a fluorescence-imaging plate reader (FLIPR) calcium kit dye (Calcium 3 kit, Molecular Devices Ltd.) containing 5 mM final probenecid and incubated at 37 °C for 1 h in a 5% CO_2 atmosphere. The fluorescence emission caused by intracellular calcium mobilization elicited by the agonist, MCH, of the expressed receptor was determined with a FLEXstation benchtop scanning and integrated fluid transfer workstation (Molecular Devices Ltd). To detect antagonists and determine compound IC_{50}, compounds were preincubated at varying concentrations with the loaded cells for 15 min at 37 °C, 5% CO_2, prior to the addition of the agonist (cold MCH-1) at its EC_{80} concentration. The fractional response values for each well were calculated as peak minus basal response. Data were calculated as the mean of triplicate wells using Excel and XL fit (Microsoft). The IC_{50} was determined as the concentration of antagonist that decreased the response to an EC_{80} concentration (0.1 μM) of agonist by 50%.

Acknowledgment. We thank BioSolveIT GmbH for supplying an evaluation copy of the FTrees program and Tripos U.K. for developing the Sybyl Programming Language script used to mutate one protein structure to another according to a specified sequence alignment.

Note Added after ASAP Posting. This manuscript was released ASAP on 7/2/2004 with an error in the designation of Asp172 in the last paragraph before the Discussion. The correct version was posted on 7/7/2004.

References

(1) Cummings, D. E.; Schwartz, M. W. Genetics and pathophysiology of human obesity. *Annu. Rev. Med.* **2003**, *54*, 453−471.
(2) Tataranni, P. A. Treatment of obesity: Should we target the individual or society? *Curr. Pharm. Des.* **2003**, *9*, 1151−1163.
(3) Weigle, D. S. Pharmacological therapy of obesity: Past, present, and future. *J. Clin. Endocrinol. Metab.* **2003**, *88*, 2462−2469.
(4) Crowley, V. E. F.; Yeo, G. S. H.; O'Rahilly, S. Obesity therapy: Altering the energy intake- and-expenditure balance sheet. *Nat. Rev. Drug Discovery* **2002**, *1*, 276−286.
(5) Chaki, S.; Nakazato, A. Recent advances in feeding suppressing agents: potential therapeutic strategy for the treatment of obesity. *Expert Opin. Ther. Pat.* **2001**, *11*, 1677−1692.
(6) Schwartz, M. W.; Woods, S. C.; Porte, D., Jr.; Seeley, R. J.; Baskin, D. G. Central nervous system control of food intake. *Nature* **2000**, *404*, 661−671.
(7) Largent, B. L.; Robichaud, A. J.; Miller, K. J. Promise and progress of central G protein-coupled receptor modulators for obesity treatments. *Annu. Rep. Med. Chem.* **2002**, *37*, 1−10.
(8) Fujisawa, Y.; Mori, M.; Ohtaki, T.; Hinuma, S.; Fujino, M. Orphan GPCR ligands related to obesity. *Curr. Med. Chem.: Cent. Nerv. Syst. Agents* **2003**, *3*, 101−120.
(9) Hervieu, G. Melanin-concentrating hormone functions in the nervous system: food intake and stress. *Expert Opin. Ther. Targets* **2003**, *7*, 495−511.
(10) Chambers, J.; Ames, R. S.; Bergsma, D.; Muir, A.; Fitzgerald, L. R.; Hervieu, G.; Dytko, G. M.; Foley, J. J.; Martins, J.; Liu, W.-S.; Park, J.; Ellis, C.; Ganguly, S.; Konchar, S.; Cluderay, J.; Leslie, R.; Wilson, S.; Sarau, H. M. Melanin-concentrating hormone is the cognate ligand for the orphan G protein-coupled receptor SLC-1. *Nature* **1999**, *400*, 261−265.
(11) Saito, Y.; Nothacker, H.-P.; Wang, Z.; Lin, S. H. S.; Leslie, F.; Civelli, O. Molecular characterization of the melanin-concentrating-hormone receptor. *Nature* **1999**, *400*, 265−269.
(12) Suply, T.; Della Z. O.; Audinot, V.; Rodriguez, M.; Beauverger, P.; Duhault, J.; Canet, E.; Galizzi, J.-P.; Nahon, J.-L.; Levens, N.; Boutin, J. A. SLC-1 receptor mediates effect of melanin-concentrating hormone on feeding behavior in rat: a structure−activity study. *J. Pharmacol. Exp. Ther.* **2001**, *299*, 137−146.
(13) Shearman, L. P.; Camacho, R. E.; Sloan Stribling, D.; Zhou, D.; Bednarek, M. A.; Hreniuk, D. L.; Feighner, S. D.; Tan, C. P.; Howard, A. D.; Van der Ploeg, L. H. T.; MacIntyre, D. E.; Hickey, G. J.; Strack, A. M. Chronic MCH-1 receptor modulation alters appetite, body weight and adiposity in rats. *Eur. J. Pharmacol.* **2003**, *475*, 37−47.
(14) Takekawa, S.; Asami, A.; Ishihara, Y.; Terauchi, J.; Kato, K.; Shimomura, Y.; Mori, M.; Murakoshi, H.; Kato, K.; Suzuki, N.; Nishimura, O.; Fujino, Mo. T-226296: a novel, orally active and selective melanin-concentrating hormone receptor antagonist. *Eur. J. Pharmacol.* **2002**, *438*, 129−135.
(15) Borowsky, B.; Durkin, M. M.; Ogozalek, K.; Marzabadi, M. R.; DeLeon, J.; Heurich, R.; Lichtblau, H.; Shaposhnik, Z.; Daniewska, I.; Blackburn, T. P.; Branchek, T. A.; Gerald, C.; Vaysse, P. J.; Forray, C. Antidepressant, anxiolytic and anorectic effects of a melanin-concentrating hormone-1 receptor antagonist. *Nat. Med.* **2002**, *8*, 825−830.
(16) Marsh, D. J.; Weingarth, D. T.; Novi, D. E.; Chen, H. Y.; Trumbauer, M. E.; Chen, A. S.; Guan, X.-M.; Jiang, M. M.; Feng, Y.; Camacho, R. E.; Shen, Z.; Frazier, E. G.; Yu, H.; Metzger, J. M.; Kuca, S. J.; Shearman, L. P.; Gopal-Truter, S.; MacNeil, D. J.; Strack, A. M.; MacIntyre, D. E.; Van der Ploeg, L. H. T.; Qian, S. Melanin-concentrating hormone 1 receptor-deficient mice are lean, hyperactive, and hyperphagic and have altered metabolism. *Proc. Natl. Acad. Sci. U.S.A.* **2002**, *99*, 3240−3245.
(17) Collins, C. A.; Kym, P. R. Prospects for obesity treatment: MCH receptor antagonists. *Curr. Opin. Invest. Drugs* **2003**, *4*, 386−394.
(18) Browning, A. Recent developments in the discovery of melanin-concentrating hormone antagonists: novel antiobesity agents. *Expert Opin. Ther. Pat.* **2004**, *14*, 313−325.
(19) McKittrick, B. A.; Su, J.; Clader, J. W.; Li, S.; Guo, G. Piperidine MCH antagonists and their use in the treatment of obesity. PCT Intl. Appl. WO 02/051809 A1, 2002.
(20) Anon. MCH-1 receptor antagonists, Synaptic. IDdb3 Drug Report. Data presented at 14th World Congress of Pharmacology in San Francisco, CA, July 2002.
(21) Lagu, B.; Wetzel, J.; Marzabadi, M. R.; Deleon, J. E.; Gluchowski, C.; Noble, S.; Nagarathnam, D.; Chiu, G. Selective melanin concentrating hormone-1 (MCH-1) receptor antagonists and uses thereof. PCT Intl. Appl. WO 02/06245 A1, 2002.
(22) Kato, K.; Mori, M.; Suzuki, M.; Shimoura, Y.; Takekawa, S.; Choh, M. MCH antagonists. PCT Intl. Appl. WO 01/21169 A1, 2001.
(23) Ishihara, Y.; Suzuki, N.; Takekawa, S. Melanin-concentrating hormone antagonists. Japanese Patent JP2001-226269, 2001.
(24) Bakthavatchalam, R.; Hutchison, A.; Thurkauf, A. Melanin-concentrating hormone receptor ligands. PCT Intl. Appl. WO 02/04433 A2, 2002.
(25) Johnson, C. N.; Jones, M.; O'Toole, C. A.; Stemp, G.; Thewlis, K. M.; Witty, D. Carboxamide compounds and their use as antagonists of a human 11cby receptor. PCT Intl. Appl. WO 02/10146 A1, 2002.
(26) McBriar, M. D.; Palani, A.; Shapiro, S. A.; Xu, R.; Clader, J. MCH antagonists and their use in the treatment of obesity. PCT Intl. Appl. WO 02/057233 A1, 2002.
(27) Sheridan, R. P.; Kearsley, S. K. Why do we need so many chemical similarity search methods? *Drug Discovery Today* **2002**, *7*, 903−911.
(28) The ClogP (v4.0) program is marketed by Daylight Chemical Information Systems Inc. (27401 Los Altos, Suite 360, Mission Viejo, CA 92691; http://www.daylight.com) and maintained and developed by Biobyte Corp. (201 W. 4th Street, No. 204, Claremont, CA 91711; http://www.biobyte.com).
(29) Ward, J. H. Hierarchical grouping to optimize an objective function. *J. Am. Stat. Assoc.* **1963**, *58*, 236−244.
(30) Arienzo, R.; Clark, D. E.; Cramp, S.; Daly, S.; Dyke, H. J.; Lockey, P. M.; Norman, D.; Roach, A. G.; Stuttle, K.; Tomlinson, M.; Wong, M.; Wren, S. P. Structure−activity relationships of a novel series of melanin-concentrating hormone (MCH) receptor antagonists. *Bioorg. Med. Chem. Lett.*, in press.
(31) Okada, T.; Fujiyoshi, Y.; Silow, M.; Navarro, J.; Landau, E. M.; Shichida, Y. Functional role of internal water molecules in rhodopsin revealed by x-ray crystallography. *Proc. Natl. Acad. Sci. U.S.A.* **2002**, *99*, 5982−5987.
(32) MacDonald, D.; Mirgolo, Z.; Durkin, J. P.; Xiaorui, Y.; Strader, C. D.; Graziano, M. P. Molecular characterization of the melanin-concentrating hormone/receptor complex: Identification of critical residues involved in binding and activation. *Mol. Pharmacol.* **2000**, *58*, 217−225.
(33) Bissantz, C.; Bernard, P.; Hibert, M.; Rognan, D. Protein-based virtual screening of chemical databases. II. Are homology models of G-protein coupled receptors suitable targets? *Proteins* **2003**, *50*, 5−25.
(34) Evers, A.; Klebe, G. Ligand-supported homology modeling of G-protein-coupled receptor sites: models sufficient for successful virtual screening. *Angew. Chem., Int. Ed.* **2004**, *43*, 248−251.
(35) Flohr, S.; Kurz, M.; Kostenis, E.; Brkovich, A.; Fournier, A.; Klabunde, T. Identification of nonpeptidic urotensin II receptor antagonists by virtual screening based on a pharmacophore model derived from structure−activity relationships and nuclear magnetic resonance studies on urotensin II. *J. Med. Chem.* **2002**, *45*, 1799−1805.

(36) Varady, J.; Wu, X.; Fang, X.; Min, J.; Hu, Z.; Levant, B.; Wang, S. Molecular modeling of the three-dimensional structure of dopamine 3 (D3) subtype receptor: Discovery of novel and potent D3 ligands through a hybrid pharmacophore- and structure-based database searching approach. *J. Med. Chem.* **2003**, *46*, 4377−4392.
(37) Schneider, G.; Nettekoven, M. Ligand-based combinatorial design of selective purinergic receptor (A_{2A}) antagonists using self-organizing maps. *J. Comb. Chem.* **2003**, *5*, 233−237.
(38) Rishton, G. M. Reactive compounds and in vitro false positives in HTS. *Drug Discovery Today* **1997**, *2*, 382−384.
(39) Rishton, G. M. Nonleadlikeness and leadlikeness in biochemical screening. *Drug Discovery Today* **2003**, *8*, 86−96.
(40) Hann, M.; Hudson, B.; Lewell, X.; Lifely, R.; Miller, L.; Ramsden, N. Strategic pooling of compounds for high-throughput screening. *J. Chem. Inf. Comput. Sci.* **1999**, *39*, 897−902.
(41) Lipkus, A. H. Exploring chemical rings in a simple topological-descriptor space. *J. Chem. Inf. Comput. Sci.* **2001**, *41*, 430−438.
(42) Available from Daylight Chemical Information Systems, Inc. (27401 Los Altos, Suite 360, Mission Viejo, CA 92691; http://www.daylight.com).
(43) Balducci, R.; McGarity, C. M.; Rusinko, A., III; Skell, J.; Smith, K.; Pearlman, R. S. (University of Texas at Austin). *Concord 4.06*; Distributed by Tripos, Inc., 1699 S. Hanley Road, Suite 303, St. Louis, MO 63144-2913; http://www.tripos.com.
(44) *Unity 4.3*; Tripos, Inc., 1699 S. Hanley Road, Suite 303, St. Louis, MO 63144-2913; http://www.tripos.com.
(45) Lemmen, C., Lengauer, T.; Klebe, G. FLEXS: A Method for Fast Flexible Ligand Superposition. *J. Med. Chem.* **1998**, *41*, 4502−4520.
(46) *FlexS 1.9*; Tripos, Inc., 1699 S. Hanley Road, Suite 303, St. Louis, MO 63144-2913; http://www.tripos.com.
(47) Ertl, P.; Rohde, B.; Selzer, P. Fast calculation of molecular polar surface area as a sum of fragment-based contributions and its application to the prediction of drug transport properties. *J. Med. Chem.* **2000**, *43*, 3714−3717.
(48) Topological PSA values were calculated using the tpsa program written by Peter Ertl and distributed as part of the "contrib." codes with Daylight software; http://www.daylight.com/support/contrib/.
(49) *Sybyl 6.8*; Tripos, Inc., 1699 S. Hanley Rd., Suite 303, St. Louis, MO 63144-2913; http://www.tripos.com.
(50) Salim, N.; Holliday, J.; Willett, P. Combination of fingerprint-based similarity coefficients using data fusion. *J. Chem. Inf. Comput. Sci.* **2003**, *43*, 435−442.
(51) *Macromodel 7.2*; Schrödinger, Inc., 1500 S. W. First Avenue, Suite 1180, Portland, OR 97201-5815; http://www.schrodinger-.com.
(52) Jones, G.; Willett, P.; Glen, R. C. A genetic algorithm for flexible molecular overlay and pharmacophore elucidation. *J. Comput.-Aided Mol. Des.* **1995**, *9*, 532−549.
(53) *GASP*; Tripos, Inc., 1699 S. Hanley Road, Suite 303, St. Louis, MO 63144-2913; http://www.tripos.com.
(54) Clark, D. E. Rapid calculation of polar molecular surface area and its application to the prediction of transport phenomena. 2. Prediction of blood−brain barrier penetration. *J. Pharm. Sci.* **1999**, *88*, 815−821.
(55) *QikProp 1.6*; Schrödinger, Inc., 1500 S. W. First Avenue, Suite 1180, Portland, OR 97201-5815; http://www.schrodinger.com.
(56) Carhart, R. E.; Smith, D. H.; Venkataraghavan, R. Atom pairs as molecular features in structure−activity studies: definition and applications. *J. Chem. Inf. Comput. Sci.* **1985**, *25*, 64−73.
(57) Rarey, M.; Dixon, J. S. Feature trees: a new molecular similarity measure based on tree matching. *J. Comput.-Aided Mol. Des.* **1998**, *12*, 471−490.
(58) *FTrees*; BioSolveIT GmbH, An der Ziegelei 75, 53757 Sankt Augustin, Germany; http://www.biosolveit.de.
(59) Furse, K. E.; Lybrand, T. P. Three-dimensional models for β-adrenergic receptor complexes with agonists and antagonists. *J. Med. Chem.* **2003**, *46*, 4450−4462.
(60) Palczewski, K.; Kumasaka, T.; Hori, T.; Behnke, C. A.; Motoshima, H.; Fox, B. A.; Le Trong, I.; Teller, D. C.; Okada, T.; Stenkamp, R. E.; Yamamoto, M.; Miyano, M. Crystal structure of rhodopsin: A G protein-coupled receptor. *Science* **2000**, *289*, 739−745.

JM040762V